

# Directional relay co-ordination in ungrounded MV radial distribution networks using a RTDS

A. A. van der Meer, M. Popov

**Abstract**— In this paper, the results of a relay co-ordination study of an existing ungrounded medium voltage (MV) network are presented. For this study, Real Time Digital Simulator (RTDS) which is a part of a closed-loop relay test system is used. The relay is a Siemens electronic directional overcurrent relay with a ground-fault element. Amplifiers are applied in order to supply the relay with its nominal secondary current and voltage.. Furthermore, sequence-components have been used for the calculation of the protection blinding zone inside the feeder cable during single phase-to-ground faults. As a result, a maximum allowable network capacitance to ground is calculated, for which all ground faults can be detected and interrupted.

**Keywords:** RTDS, overcurrent relay, directional protection, RTDS

## I. INTRODUCTION

CURRENTLY more than ever, electricity companies tend to optimize their asset management strategy. A clear power system protection concept plays an important role within this strategy. Medium voltage (MV) distribution networks were initially left ungrounded because the need for higher basic insulation coordination was inferior to the advantage of continuous circuit operation during single phase-to-ground faults [1]. Distribution networks continue to expand however and so do zero-sequence fault-currents. Moreover, temporary overvoltages (up to 3.5 p.u.) can be present during single phase-to-ground faults [2]. It is very expensive to invest in better neutral-grounding methods however, and therefore much efforts have been done to optimize existing relaying methods.

RTDS technology originated in the mid 1990's as there was a growing need for fast power system simulation studies [3][4]. RTDS is extensively used nowadays in closed-loop protective relay testing and system studies for which real-time operation is required [5]-[8].

This paper presents a relay coordination method for the protection against single phase-to-ground faults of 2 parallel feeder cables in a MV ungrounded distribution network. The protection method relies on overcurrent and directional protection by making use of the zero-sequence quantities of

the voltages and currents. Boundary conditions are presented by generalizing the fault current calculation for several values of the MV network cable capacitances.

Section II describes a simplified network model simulated in both MATLAB and RTDS. The applied fault calculation method is described briefly. Section IV presents the basic operation of unidirectional and directional relays as it is used in practice in closed-loop operation. Minimum relay settings are determined and a current margin factor  $\alpha$  is introduced. Simulation results for both, RTDS and MATLAB are presented in Section V. The presence of a death-zone (DZ) is calculated and discussed. The work is outlined by a practical example.

## II. NETWORK DESCRIPTION

The analyzed network is shown in Fig. 1, which is a simplification of a typical ungrounded 10 kV network which is extensively utilized in the Netherlands.

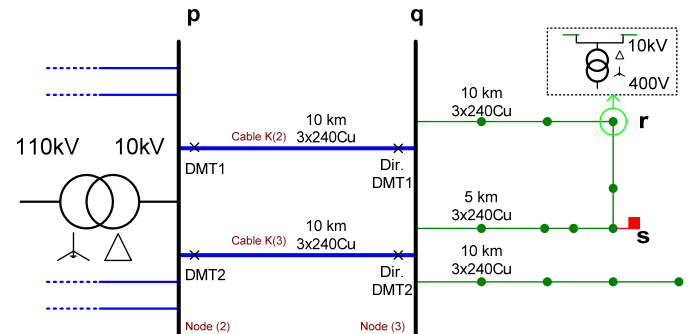


Fig. 1: Typical ungrounded MV network with two feeder cables.

The coordination study focuses on single phase-to-ground faults inside the two parallel feeder cables. The MV network is connected to the parallel voltage (HV) network at the HV/MV substation (p). From here, feeder cables (between p and q) supply MV distribution substations (q), from where the power is transported further to the low voltage (LV) side by distribution cables (right to q) and distribution transformers (r). Some distribution cables lie in a circular way in order to be manually interconnected in case of an emergency (s). Definite minimum-time relays (DMT1 & DMT2) are positioned at the substation side of cable K(2) and cable K(3). Directional relays (Dir. DMT1 & Dir. DMT2) are placed at the end of the feeder cables. The network of Fig. 1 is further simplified by aggregating the cables' distributed capacitances to one lumped capacitance, as shown in Fig. 2.

A.A. van der Meer and M. Popov, are with the Delft University of Technology, Faculty of Electrical Engineering, Mathematics and Informatics, Mekelweg 4, Delft 2628CD, The Netherlands, (e-mail: [A.A.vanderMeer@tudelft.nl](mailto:A.A.vanderMeer@tudelft.nl), [M.Popov@tudelft.nl](mailto:M.Popov@tudelft.nl)).

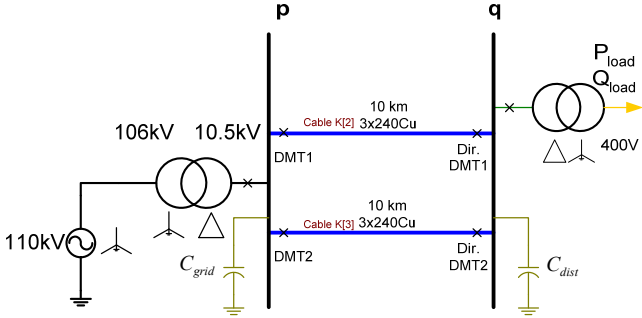


Fig. 2: Ungrounded MV grid with aggregated load and cable capacitances.

Distribution cables between q and s are represented by their capacitance to ground at node q by

$$C_{dist,0} = \sum_{n=q}^{distribution\ cable} C_{g,n} \quad (1)$$

where  $C_{g,n}$  is the capacitance to ground for the  $n^{\text{th}}$  cable section of the distribution cable on the right-hand side of q. Cables located left from node p are represented by their aggregated capacitance to ground at node p by

$$C_{grid,0} = \sum_{n=p}^{MV\ grid} C_{g,n} \quad (2)$$

Similar equations hold for the positive-sequence capacitance

$$C_{dist,1} = \sum_{n=q}^{distribution\ cable} C_{g,n} + 3C_{k,n} \quad (3)$$

$$C_{grid,1} = \sum_{n=p}^{MV\ grid} C_{g,n} + 3C_{k,n} \quad (4)$$

where  $C_{k,n}$  is phase-to-phase capacitance for each cable section of the distribution cable and the rest of the cables left from the node p respectively. This is allowed because

- The fault current is produced by the charging currents of the cables' distributed capacitances only;
- Relay operation is based on RMS-value measurements and thus, for the sake of simplicity, lumped capacitances have been used instead of distributed parameters, and
- The error introduced by using lumped capacitances instead of distributed parameters is very small for ground faults in ungrounded networks.

For other types of short circuits however, a  $\pi$ -equivalent circuit is more suitable as the fault current is dependent on the short-circuit ratio of the MV network.

Feeder cables are modeled by  $\pi$ -equivalents. The load which is on the right from the node q has negligible influence on the zero-sequence fault current, hence it is aggregated to one load directly connected to node q. The load left from the node p is neglected since it has little influence on the fault current amplitude and phase angle at node q. Transformers are modeled by leakage impedances, and the load by a lumped element. Sequence networks and the network parameters are given in the Appendix.

### III. FAULT CALCULATION METHOD

Fault calculation is done with Matlab. Fig. 3 shows the steps to be taken for correct fault calculation. First, the  $Z_{bus}$  matrices of the three sequence networks must be determined [11]. Second, prefault sequence voltages  $V_{012}^{t-1}$  are estimated by loadflow calculation. Third, the sequence voltage change  $\Delta V_{012}^{t-1}$  caused by the fault-current  $I_f$  flowing into the fault has to be calculated. This should be superposed to the prefault voltages to obtain the sequence node-voltages  $V_{012}^t$ . Finally, cable sequence-currents  $I_{mn,012}$  and phase-currents  $I_{mn,abc}$  should be calculated to simulate the relay operation correctly.

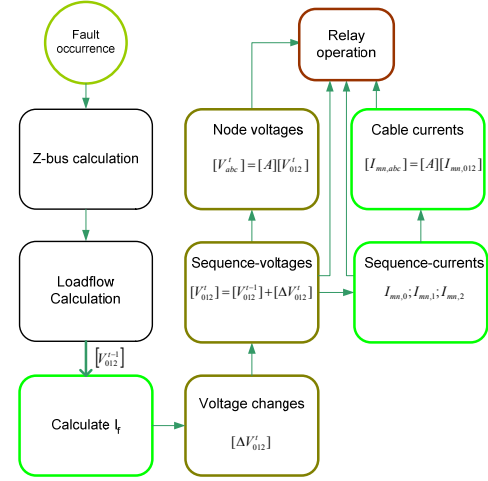


Fig. 3: Fault calculation diagram.

### IV. RELAY OPERATION

#### A. Directional relay ground-fault element operation

For ungrounded systems, it is not convenient to detect single phase-to-ground faults by using phase-currents only. During ground-faults, the combination of load current and capacitive fault current is measured. The direction of ground faults should therefore be determined by an earth-fault element, that uses zero-sequence components  $\underline{U}_0$  and  $I_{e,relay} = -3I_0$  as phasor quantities [9].  $\underline{U}_0$  will be used as a reference phasor, which is rotated by an angle  $RCA_0$  to make a distinction between forward and backward faults as depicted in Fig. 4.

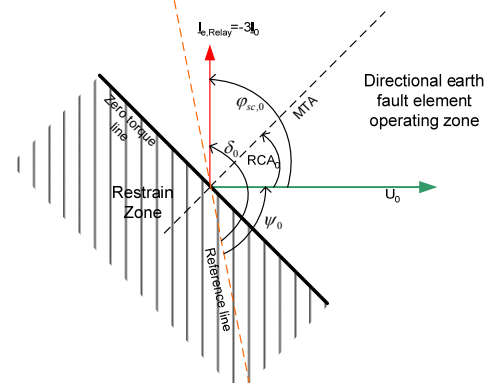


Fig. 4: Operating and restrain zone for a typical directional earth-fault element.

For the measured zero-sequence power to detect a forward ground-fault holds:

$$P_0 = \text{Re}\left(\underline{U}_0 e^{jRCA_0} \underline{I}_{e,relay}^*\right) = \text{Re}\left(U_0 e^{j\psi_0} e^{jRCA_0} I_{e,relay} e^{-j\delta_0}\right) \quad (5)$$

$$= U_0 I_{e,relay} \cos(\varphi_{sc,0} - RCA_0) > 0$$

where  $\varphi_{sc,0}$  the angle between  $\underline{U}_0$  and  $\underline{I}_{e,relay}$  during unbalanced conditions,  $RCA_0$  the zero sequence relay characteristic angle,  $\psi_0$  the phase angle of  $\underline{U}_0$  and  $\delta_0$  the phase angle of  $\underline{I}_{e,relay}$ . It should be noted that the currents are measured as they flow *into* the cable, which results in a zero sequence current  $\underline{I}_0$  lagging  $\underline{U}_0$  by  $90^\circ$ . Two conditions should be fulfilled to trigger the directional earth-fault element pick-up/drop-off timer. First, the RMS-value of  $\underline{I}_{e,relay}$  must be higher than the pick-up value before a forward direction can be determined.

### B. Relay settings

Earth-fault element minimum relay settings are determined by the charging current of the distribution cables (beyond node q in Fig. 1). A ground fault in cable K(3) should cause DMT2 or Dir. DMT2 to trip. Thereafter, the capacitive fault current flows partly through the healthy feeder cable towards the faulted cable, causing the other relay to trip. Now, the ground-fault is isolated and the faulted cable has been interrupted selectively. During this period, the healthy cable carries the full distribution cable capacitive charging current  $I_{e,dist}$  (in case Dir. DMT2 trips) or the remaining MV-network capacitive charging current  $I_{e,grid}$  (in case DMT2 trips). Moreover, DMT2 and the unidirectional element of Dir. DMT2 also measures the charging current of cable K(2),  $I_{e,cable}$ . The cable protection must not respond to these currents. Table I shows the minimum earth-fault element settings for both DMT and Dir. DMT relays. For  $I_{e,dist}$  holds

$$I_{e,dist} \approx 3U_{q,0} \omega C_{dist,0} \quad (6)$$

where  $U_{q,0}$  is the zero-sequence voltage during a single phase-to-ground fault,  $\omega$  the radial frequency and  $C_{dist,0}$  the distribution cable aggregated capacitance [10]. Consequently holds for  $I_{e,cable}$

$$I_{e,cable} \approx 3U_{p,0} \omega C_{cable,0} \quad (7)$$

with  $U_{p,0}$  the zero-sequence voltage at node  $p$ . The settings shown in Table I are the minimum relay pick-up settings. Every network topology change would make adjustment of the relay settings necessary. Therefore, a margin factor  $\alpha$  is introduced to prevent undesirable, uncoordinated circuit interruptions. Applying a too high margin can result in a death-zone (DZ) area within the cable, an area in which ground-faults will not be detected. Table II shows the minimum earth-fault settings including the proposed margin factor  $\alpha$ .

TABLE I  
EARTH-FAULT ELEMENT MINIMUM PICK UP SETTINGS

Current Setting	Application	Overcurrent
Dir. DMT $+I_{e>}, +t_{e>}$	Dir. DMT earth-fault element pick up current and time	$I_{e,dist} > 0.3s$
DMT $I_{e>}, t_{e>}$	DMT earth-fault element pick up current and time	$I_{e,dist} + I_{e,cable} > 0.9s$

TABLE II  
EARTH-FAULT ELEMENT MINIMUM PICK UP SETTINGS INCLUDING  $\alpha$

Relay Setting	Value
Dir. DMT $+I_{e>}, +t_{e>}$	$\left(1 + \frac{\alpha}{100}\right) \cdot I_{e,dist} > 0.3s$
DMT $I_{e>}, t_{e>}$	$\left(1 + \frac{\alpha}{100}\right) \cdot I_{e,dist} + I_{e,cable} > 0.9s$

### C. Closed-loop operation

The implementation of an external relay is done according to Fig. 5. The connected 7SJ62 directional relay replaces Dir. DMT2 of Fig. 2 during real-time operation. At the workstation, a short-circuit current can be ignited by the runtime environment. The relay trip contact is connected to the digital input of the RTDS which establishes a closed-loop system. The voltage and current signals, which are created at the analogue output of the RTDS, must be amplified to nominal secondary voltages and currents, to let the relay work properly. The applied amplifiers are Quad 50E audio amplifiers which are connected in wye in order to simulate the secondary circuit as realistic as possible. Toroidal transformers have been added to the current amplifiers to produce correct rated secondary currents. The trip contact of the relay is connected to the RTDS in which a virtual switch triggers during the simulation. The operation of the amplifier has been verified at KEMA T&D, Arnhem, the Netherlands. Fig. 6 shows the verification of the zero-sequence current amplification as measured by the relay for both Quad 50E amplifiers and KEMA amplifiers. Although some differences exist, the Quad 50E amplifiers provide correct relay operation: The direction and the RMS-value are determined correctly. Fig. 7 shows the closed-loop test setup used during the relay co-ordination study.

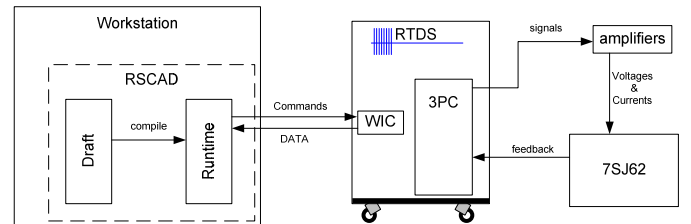


Fig. 5: Closed-loop operation of a 7SJ62 directional relay (right) .A workstation is needed to adjust operation constraints in real-time (left).

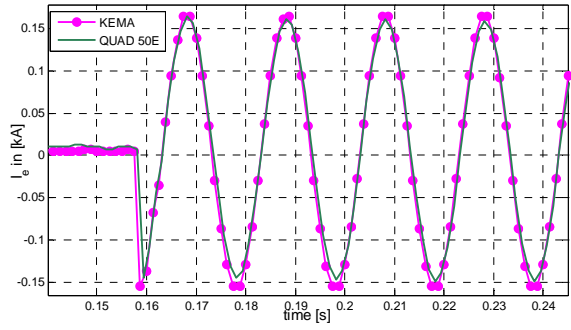


Fig. 6: Earth return path current as measured by the directional relay for both the Quad 50E amplifiers and the sophisticated amplifiers of KEMA.

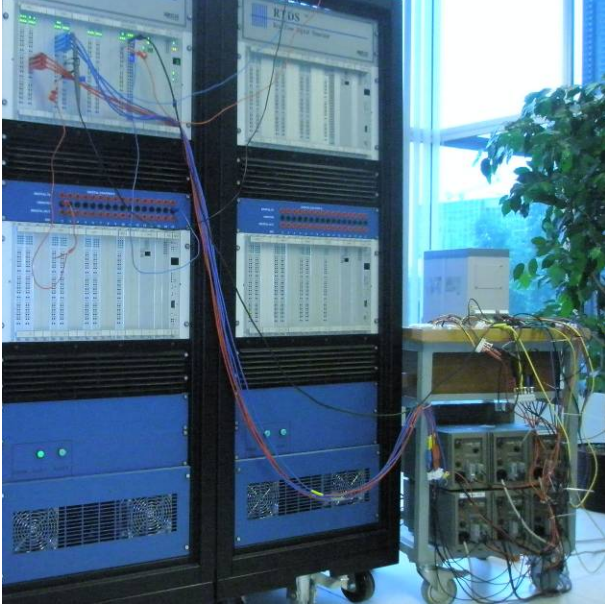


Fig. 7. Closed-loop relay test circuit.

## V. SIMULATION RESULTS

### A. Correct cable interruption

Correct relay co-ordination is satisfied only if

$$I_{e,Dir DMT} > I_{e>} \cup I_{e,DMT} > I_{e>} \quad \forall k \in \{0..1\} \quad (8)$$

where  $I_{e,Dir DMT}$  the earth-fault current measured by the directional overcurrent relay,  $I_{e,DMT}$  the earth-fault current measured by the overcurrent relay and  $k$  the fault location in per-unit cable-length. This means that at least one relay that protects the feeder cable should pick up during a single phase-to-ground fault inside the feeder cable. Table III shows the relay settings for the given network.

Fig. 8 shows the waveforms of a single phase-to-ground fault being interrupted correctly by the 7SJ62 and RTDS.

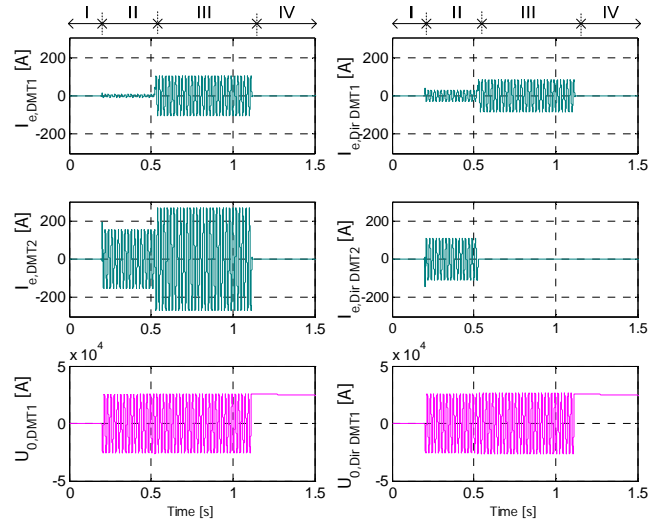


Fig 8: Correct circuit interruption after a single phase-to-ground fault. Upper left and right graphs represent earth-fault current measured by the relays protecting cable K[2]; Centre left and right graphs represent earth-fault currents as measured by the relays protecting cable K[3]. Bottom graphs show the zero-sequence voltage at node p and q during a single phase-to-ground fault.

Only zero-sequence quantities are shown as the phase elements of all four relays do not respond to the small fault current. Basically, the fault interruption contains four steps:

I pre-fault voltages and currents: The system is in steady state as a balanced set of voltages and currents are present. Therefore, no zero-sequence quantities occur.

II fault ignition: A single phase-to-ground fault is initiated in the centre ( $k=0.5$  per unit) of cable K[3] at  $t=0.20$  s. Zero-sequence currents are measured by the relays as the system is unbalanced. Both DMT2 and Dir. DMT2 pick up by the measured earth-fault current flowing towards the fault. The directional relay needs one period for the direction determination and it will eventually trip at  $t=0.52$  s, interrupting the cable at one side. Dir. DMT2 is part of the closed-loop system, hence a small trip delay was expected, which is common in practical situations as well.

III DMT2 interruption: During this period, cable K[3] is connected to the grid by node p only, making it evident that the earth-fault current can flow only from one side. The earth-fault element of DMT2 had already been triggered in period II and trips after another 0.6 s. at  $t=1.12$  s. During this period,  $I_{e,dist}$  flows through cable K[2] and both relays may not pick up on this current.

IV Post-fault situation: at  $t=1.12$  s, the faulted cable is interrupted and the system restored from unbalanced operation. This yields that, at the fault clearing time instant, the charging current of the cleared phase recovers while the capacitances of the healthy phases are fully charged and the charge is trapped inside the cable. This leads to a symmetrical three-phase voltage system with a direct voltage component of  $\sqrt{2}U_{phase}$  which gradually increases or decreases, seriously stressing the cable isolation [10]. This residual voltage can be observed as a DC-component in the zero-sequence waveforms. In this case, both relays picked up after fault initiation. Other fault locations would possibly yield only one relay to pick up.

### B. Death-zone calculation

When no relay picks up at all during a single phase-to-ground fault, a DZ is present. To determine whether a DZ is present in a cable or not,  $C_{dist,0}$  was varied and  $C_{grid,0}$  was held fixed as single phase-to-ground faults were simulated at equally distributed locations in cable K[3].

Fig. 9 shows the occurrence of a DZ while varying  $C_{dist,0}$  and hence  $\mu = \frac{C_{dist,0}}{C_{grid,0}}$  for fault location intervals of 100 m. (0.02 pu). Since the relay settings change during variation of  $C_{dist,0}$  as well, both DMT and Dir. DMT settings are spanning 2 parallel planes. When for a given value of  $\mu$  and  $k$  (8) does not hold, a DZ is present. Only the lowest value of  $\mu$ ,  $\mu_{lim}$ , is important for correct relay co-ordination while this value corresponds to the maximum allowable cable capacitance (and hence cable length) installed beyond node q.

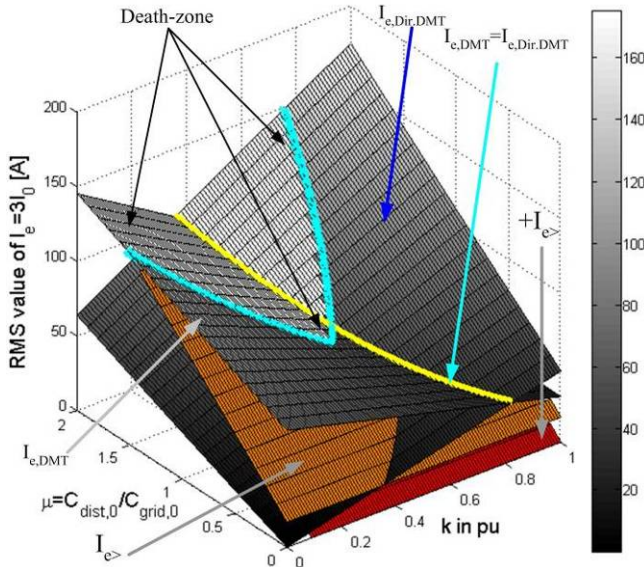


Fig. 9: Presence of a death-zone during a single phase-to-ground-fault in cable K[3] as the fault location  $k$  (in pu) and the network capacitance factor  $\mu$  are varied. Earth-fault currents measured at both cable ends are depicted as two planes crossing each other at the indicated line.  $I_{e^-}$  and  $+I_{e^+}$  settings vary with  $\mu$ , spanning two parallel planes.

### C. General death-zone calculation

The DZ calculation shown in Fig. 11 is valid for the given network only. No conclusions can be drawn about the maximum allowable capacitance  $C_{dist,0,lim}$  for other values of  $C_{grid,0}$ . Therefore, the calculations are generalized by taking the variation of  $C_{grid,0}$  into account as well. Fig. 10 shows the values of  $\mu_{lim}$  as a function of  $C_{grid,0}$  for  $\alpha=0$ ,  $\alpha=25$ ,  $\alpha=40$  and  $\alpha=50$ . It can be observed that, for approximately  $5 \mu\text{F} \leq C_{grid,0} \leq 35 \mu\text{F}$ ,  $\mu_{lim}$  is constant and hence invariant of  $C_{grid,0}$ . The average value of  $\mu_{lim}$  for  $\alpha=25$  at the interval  $5 \mu\text{F} \leq C_{grid,0} \leq 35 \mu\text{F}$  is  $\mu_{lim}=0.86$ . Calculations are performed by varying  $C_{dist,0}$  and  $C_{grid,0}$  whilst the feeder cable length is kept fixed. It turned out that the variation of the cable length results in small variations of the average values of  $\mu_{lim}$ .

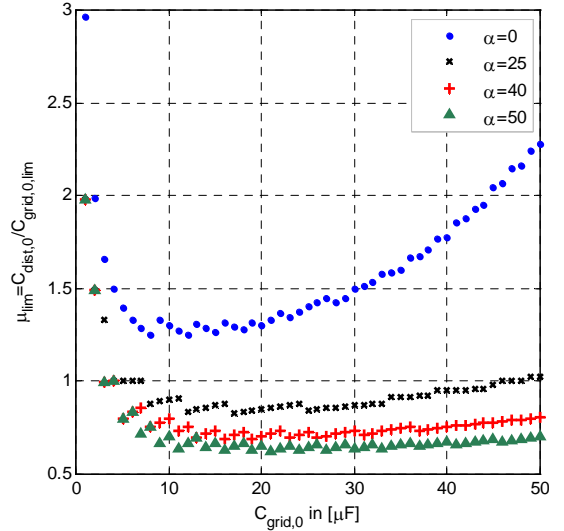


Fig. 10:  $\mu_{lim}$  as a function of  $C_{grid,0}$  for  $\alpha=0$ ,  $\alpha=25$ ,  $\alpha=40$  and  $\alpha=50$ .  $C_{grid,0}$  was varied with steps of  $1 \mu\text{F}$  during the simulation.

## VI. CONCLUSIONS

This contribution presented a detailed relay coordination study. Single phase-to-ground faults have extensively been studied and a protection method for single phase-to-ground-faults in ungrounded cable networks has been established. The method can be used generally for radial cable networks. For the discussed network, the following can be concluded:

- For a limited range of network capacitance,  $\mu_{lim}$  is equal to 0.86;
- The method has only been applied for two parallel cables. More parallel cables should lead to less critical protection coordination;
- All phase-to-ground faults in the MV network should be switched off selectively;
- For the given network, a maximum  $C_{dist,0}$  of  $17 \mu\text{F}$  can be applied for correct relay co-ordination;

The study presented here shows that the RTDS can be used with full success for protection studies because relays can interact with the circuit as they do in practice as well. Amplifiers are needed for correct amplification of voltage and current signals.

It can be questioned if a DZ situation would occur in practice: the sum of the distribution cables on the right from node  $q$  is as long as the sum of the cables on the left from node  $p$ . Moreover, extensive distribution networks are meshed in practice which makes a sophisticated protection strategy necessary.

Although not simulated, a remote phase-to-ground fault in a distribution cable on the right from the node  $q$  will usually cause the DMT relays to pick-up by the fault current caused by  $C_{grid,0}$ . Therefore, all ground faults located *beyond* node  $q$  should be interrupted *before* the feeder cable DMT relays do so. This is a serious extension of the proposed relay coordination method: DMT relays with proper current and time discrimination should be installed at node  $q$  for every

distribution cable.

## VII. APPENDIX

TABLE III  
NETWORK PARAMETERS AS REFERRED TO THE MV SIDE

Parameter	Value
$E_{source}$	6.29 kV
$Z_{s,0}; Z_{s,1}; Z_{load,0}; Z_{T2,0}; R_{shunt}$	1e-6 $\Omega$
$Z_{T1,0}$	2.7+j33.4 $\Omega$
$Z_{T1,1}$	1.348+j40.87 $\Omega$
$C_{grid,0}$	20e-6 F
$C_{grid,1}$	36.4e-6 F
$C_{dist,0}$	10e-6 F
$C_{dist,1}$	18.21e-6 F
$C_{cable1,0}; C_{cable2,0}$	2.8e-6 F
$C_{cable1,1}; C_{cable2,1}$	5.1e-6 F
$Z_{cable1,0}; Z_{cable2,0}$	10.97+j1.1 $\Omega$
$Z_{cable1,1}; Z_{cable2,1}$	0.79+j0.76 $\Omega$
$Z_{load,1}$	5.833+j12.04 $\Omega$
$Z_{T2,1}$	0.2205+j1.9845 $\Omega$
$f$	50 Hz

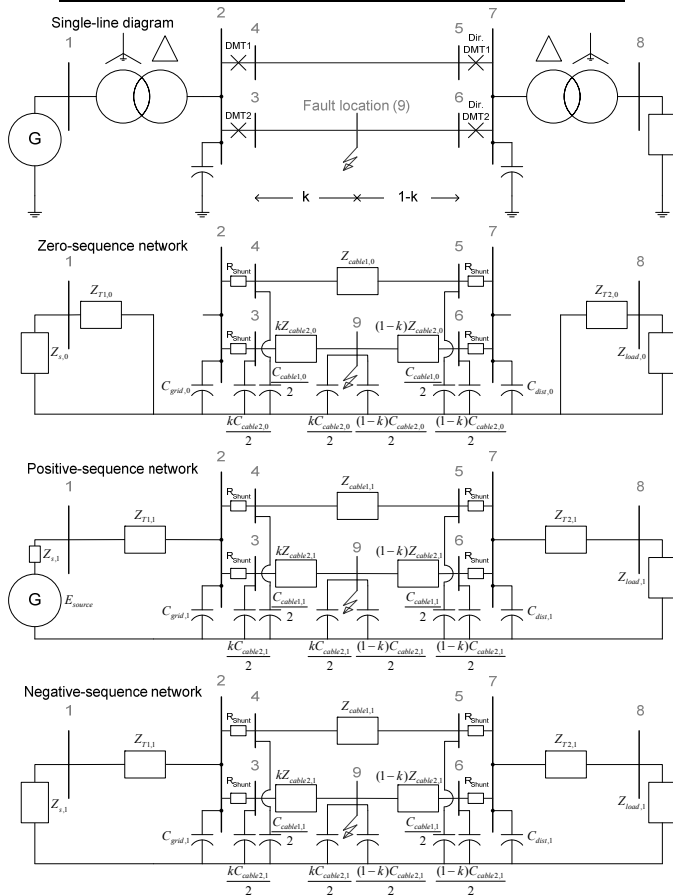


Fig. 11: Sequence networks for the aggregated network shown in Fig. 2

## VIII. REFERENCES

[1] D.L. Love, N. Hashemi: "Considerations for Ground Fault Protection in Medium-Voltage Industrial and Cogeneration Systems", *IEEE Transactions on Industry Applications*, Vol.24, no. 4, July/August 1988, pp. 548-553.

[2] F.M. Gatta, A. Geri, S. Lauria, M. Maccioni, "Analytical prediction of abnormal temporary overvoltages due to ground faults in MV networks", *Electric Power Systems Research*, Vol.77, Issue 10, August 2007, pp.1305-1313.

[3] R. Kuffel, J. Giesbrecht, T. Maguire, R.P. Wierckx, P.G. McLaren, "Fully digital power system simulator operating in real time", *Canadian Conference on Electrical and Computer Engineering*, 1996, pp.733-736.

[4] P. Forsyth, T. Maguire, R. Kuffel, "Real time digital simulation for control and protection system testing", *PESC Record - 35th IEEE Annual Power Electronics Specialists Conference*, 2004, pp. 329-335.

[5] S.F. Roekman, M. Al-Tai, S.B. Tennakoon, A. Perks: "Advanced real-time digital simulator for assessing the high performance of numerical distance relays in the Indonesian 500 kV transmission line system", *39th International Universities Power Engineering Conference*, UPEC 2004, pp.717-721.

[6] B. Wang, X. Dong, Z. Bo, A. Perks, "RTDS Environment Development of Ultra-High-Voltage Power System and Relay Protection Test", *IEEE Transactions on Power Delivery*, Vol.23, no. 2, April 2008, pp. 618-623.

[7] J. Kim, M. Park, M.H. Ali, J. Cho, J. Yoon, S.R. Lee, I. Yu, "RTDS analysis of the fault currents characteristics of HTS power cable in utility power network", *IEEE Transactions on Applied Superconductivity*, Vol.18, no. 2, June 2008, pp.684-668.

[8] D.X. Du, H.G. Wang, Z.Q. Bo, Z.X. Zhou, X.Z. Dong, B.R.J. Caunce, A. Klimek, "Design of a Real Time Digital Simulation System for Test of New Protection Schemes", *Proc. Of PowerCon 2006, International Conference on Power System Technology*, 22-26 October 2006.

[9] J. Horak, "Directional overcurrent relaying (67) concepts", *Proc. of 59th Annual Conference for Protective Relay Engineers*, 2006, pp.164-176.

[10] R. Willheim, M. Waters: "Neutral grounding in high voltage transmission", Elsevier publishing company, 1956.

[11] O.I. Elgerd, "Electric Energy Systems Theory: an introduction", McGraw-Hill series in electrical engineering, January 1982.